

A Simple Mechanical Pitch To Stall Speed Control Mechanism For A Horizontal Axis Wind Turbine (HAWT)

Abdulmalik Musa Gusau^{#1}, Abdussalam Mamoon^{*2}, Sulaiman Musa^{#3}

<sup>#Principal Technologist¹, Mechanical Engineering Department,
Kaduna Polytechnic, Kaduna, Nigeria</sup>

<sup>#Lecturer 1,² Mechanical Engineering Department, Kaduna
Polytechnic, Kaduna, Nigeria.</sup>

<sup>#Chief Lecturer³, Electrical Engineering Department, Kaduna
Polytechnic, Kaduna, Nigeria.</sup>

Abstract - A mechanism that generates a centrifugal force to mechanically pitch to stall a horizontal axis wind turbine was designed and manufactured. It comprises a projected mass that swivels in a ball joint which is fixed to the turbine rotor. The projected mass carries a sliding block that transverses along its length as it swivels, and has a slotted part which transfers the swivel action of the projected mass to the base of a rotor blade through a blade link, such that a rotary motion of the blade about its axis is achieved to stall the turbine by increasing the angle of attack of the airfoil through decreasing the pitch angle from its optimal value. The mechanism was mounted to each blade of a prototype two-blade HAWT for a performance test below and above the rated wind speed of 11 m/s in a laboratory wind tunnel. The incoming wind speed, rotor speed, generator output current, and voltage were measured during the test. The pitch to stall power curve plotted from the experimental data showed that the turbine stalled at about 11 m/s wind speed with a maximum rotor speed of 271 rpm as against 300 rpm when tested without the control mechanism. The pitch angle at the stall point as indicated in the SolidWorks motion analysis simulation result has changed from the optimal value of 35° to 15°. This simple speed control mechanism has therefore limited the rotational speed of the HAWT thereby capable of preventing it from catastrophic failure during extremely high wind conditions.

Keywords — Angle of Attack, Centrifugal Force, HAWT, Rotor Blade, Pitch to Stall

I. INTRODUCTION

The global quest of reducing CO₂ emission is one of the modern-day challenges and a viable method is the use of abundant renewable energy sources instead of fossil fuels [1]. These renewable energy sources are expected to be the alternative energy sources for power, due to the looming depletion of these fossil fuels in the future [2]. Some of the main renewable energy sources include hydropower, solar

energy, wind energy, and bioenergy among others [3]. Wind energy available around the globe is reported to be much greater than the world's energy consumption. Archer and Jacobson 2005 [4] reported that the generation potential of wind power is over five times the world's energy use in all forms, thereby making it among the fastest-growing renewable energy source.

Li *et al.*, 2012 [5] reported that horizontal wind turbines are the least expensive and clean way of harnessing this very important energy source. However, the speed at which a wind turbine rotates requires precise control and regulation below a defined limit for the safe operation of the wind machine. The absence of a speed control device on a wind turbine can cause catastrophic failure of the electrical components and mechanical damage of the turbine structure in the presence of a wind gust. Turbines are designed to safely operate up to a nominal wind speed which the control system is extremely sensitive to, and prevents the rotor from exceeding or operating above such limit.

One of the basic ways of making this protection is by “blade pitch” from which the active stall control method is achieved. As the rotor increases in speed, the blade turns to a less efficient aerodynamic angle [6]. The blade stalls, thus decreasing lift and limiting the rotor speed. When this phenomenon is achieved by decreasing the blade's angle of attack the method is called pitch control. But when it is done by increasing the angle of attack it is rather called “active stall control” [7]. Stall control can also be accomplished without blade pitching – passive stall control, by slightly twisting the blade along its longitudinal axis, such that at higher wind speed above the rated value the twisted part of the blade experiences a turbulence flow of wind which tends to stall the rotor assembly [8]. Comparatively, power output is better controlled in the active stall system than the passive stall system at the start of a wind gust, since the rated power of the turbine generator can be achieved at high wind speeds [9].



In the recent decade, a variety of research has been conducted to design and develop a model to maximize the capture of wind energy at low wind speeds and alleviate the loading at high wind speeds with variable speed and pitch regulated mechanism. Venkaiah and Sarkar 2019 [10] developed a model-free fuzzy feedforward controller for pitch control application on HAWT through an electrohydraulic pitch actuation system. Similarly, Xu et al., 2019 [11] developed an optimal blade pitch function based on optimal blade pitch angles by using a hybrid double-disk, multiple stream-tube models. The developed model showed a significant increase in the maximum power coefficient thereby demonstrating that the blade pitch control device is feasible, functional, and effective.

This work is aimed at developing a simple mechanical device that uses a spring-operated mechanism, requiring no external energy source, that can serve as an over-speed control mechanism for a horizontal axis wind turbine. In a spring-operated mechanism, the higher rotational speed of the rotor assembly generates a centrifugal force on a regulating balancing weight that compresses the spring. The force of the weight rotates the blade about its longitudinal axis thereby increasing or decreasing the angle of attack of the airfoil to the natural incoming wind and consequently reducing the speed of the rotor assembly [9].

A successful operation of this device would positively influence local manufacturers of wind machines in Nigeria, which observes wind speeds of up to 18m/s in some regions [12], and also in other developing countries where this field of renewable energy looks largely untapped due to the inability of so many past locally attempted wind machines to last beyond few months of installations, as a result of failure and destructions from heavy wind gust during the rainy/winter seasons.

II. MATERIALS AND METHODS

Two blades each with an integral camshaft to their base, as shown in figure 1 below were machined from wooden material, and located on a rotor opposite each other through ball bearings, so that they can be rotated about their axes. A special cam profile which gives a horizontal spring-loaded follower, a linear displacement of 5mm was generated on the camshaft at a constant radius. This guides the radial motion of the blades, about their axes, between the optimum pitch angle of 35° and the lowest pitch angle of 0°.

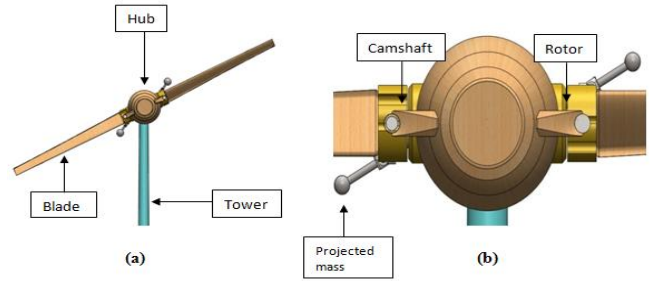


Figure 1: (a) & (b) Two-blade HAWT (front view).

A projected mass of 74 g with a rotational radius of 90mm from its center of gravity, carrying a slider mechanism along its shaft is pivoted on the face of the rotor from behind such that it swivels about a ball joint fixed to the rotor as shown in figure 2 and 3 below.

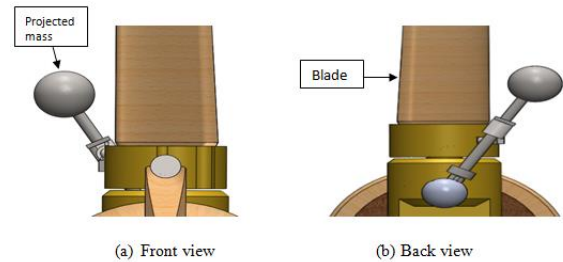


Figure 2: (a) & (b) Projected mass with the blade at the critical angle of attack

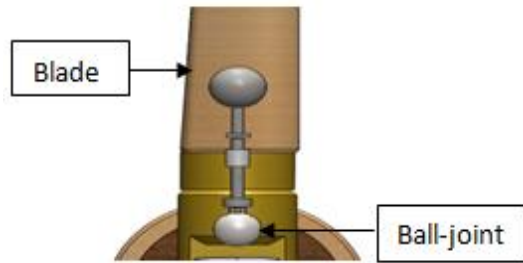


Figure 3: projected mass with the blade at a maximum angle of attack (back view).

Centrifugal forces generated on the masses due to higher speeds of rotation of the rotor cause the projected masses to swivel and rotate the blades about the blades’ axes through the slider mechanisms and blade links assemblies.

The spring-loaded followers locate and position the blades at the critical angle of attack when the turbine is at rest or rotates below its rated wind speed as shown in figure 4 below.

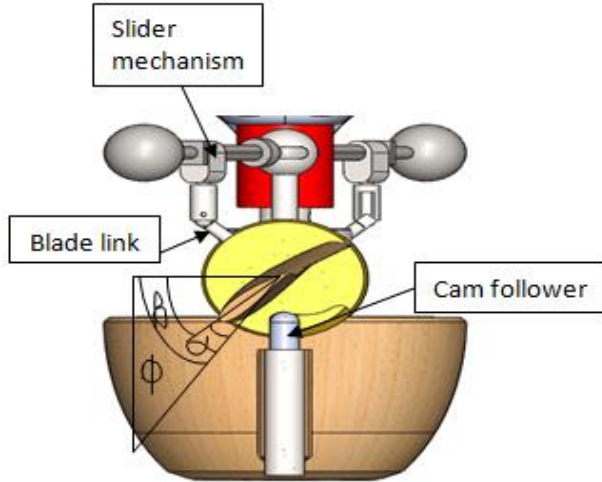


Figure 4: Turbine at rest or lower rpm (top view)

Under excessive wind conditions above the rated wind speed, the projected masses generate sufficient forces that can overcome the springs force that press the followers against the cam profiles of the blades. This effect consequently turns the blades through the pitch angle to increase the angle of attack towards the maximum as indicated in fig.5, which therefore causes the turbine to stall and rotate at a slower speed as the lift to drag coefficient begins to decline after reaching a maximum value at a threshold, although there is a significant increase in the wind speed [13].

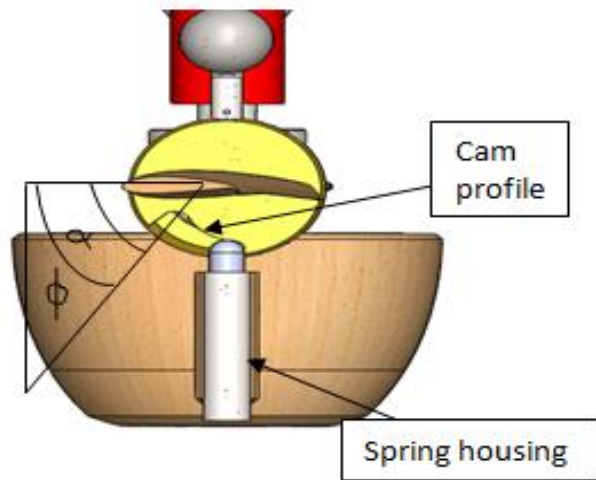


Figure 5: Turbine under excessive wind condition (top view)

The table below contains some important parameters of the wind turbine:

Table 1: Parameters of Wind Turbine

Entry	Property
ROTOR	
Airfoil	NACA 9912
Number of blades	2
Blade length	0.4m
Rotor diameter	0.87m
Hub height	2m
GENERATOR	
Type	Permanent magnet DC
Maximum voltage	40 v
Maximum current	20 Ma
Minimum speed	1000 rpm
PROJECTED MASS	
Mass	0.0741 kg ≈ 74 g
Circle radius	0.09 m
SPRINGS	
Type	Compression coil spring
Wire diameter	0.6 mm
Mean diameter	11 mm
Number of active coils	10
Free length of spring	64 mm
Pretension length	37.5 mm
Stroke	5 mm

The turbine was modeled using Solidworks design software. And the rotor assembly of the prototype was constructed from wood material.

Experiment no.1 was carried out on the turbine in a wind tunnel with an overall dimension of 1.5 m × 3 m × 7.6 (5 ft × 10 ft × 25 ft), to determine the optimal pitch angle at the rated wind speed of 11 m/s, since this angle primarily depends on the wind speed, before the cam profile that confines the blades' pitch motion between the maximum and minimum limits of 35° and 0° pitch angles respectively, was machined on the blades' camshafts [14].

The design considerations looking at the table of results from experiment no. 1 were aimed at pitching the blades to the maximum angle of attack where the pitch angle is 0° when the rotor speed exceeds 250 rpm and approaches 300 rpm, while connected directly to a DC generator.

Therefore to achieve the pitch to installation on the rotor blades, mathematical equations that relate the centrifugal force generated by a projected mass at 250 rpm and 300 rpm of the rotor assembly, to the weight of the projected mass and the spring pretension force was developed for both rise and fall conditions of a rotor blade as follows:

Condition 1: blade rise

For the blade to pitch at rising, the centrifugal force generated by the projected mass attached to the blade, F_c and the weight of the projected mass, W_t must be greater than the retention force, F_s of the spring i.e.

$$F_c + W_t > F_s$$

Or,

$$F_c + W_t = F_s + F_R.$$

$$F_R = F_c + W_t - F_s \text{ ---- (1)}$$

F_R is the magnitude by which the sum of F_c and W_t is greater than F_s .

Condition 2: blade fall

For a blade to pitch at fall the centrifugal force generated on the projected mass linked to the blade must be greater than the weight of the projected mass W_t , and the pretension force of the spring F_s put together.

I.e. $F_c > (W_t + F_s)$ or,

$$F_c = W_t + F_s + F_F.$$

$$F_F = F_c - W_t - F_s \text{ ---- (2)}$$

F_F is the magnitude by which the F_c is greater than the sum of W_t and F_s .

Positive or negative values of F_R and F_F indicate availability/unavailability of surplus forces to pitch the blade during rising and falling conditions respectively.

The centrifugal force generated on the projected masses was calculated by the following relationship:

$$F_c = m\omega^2. \text{ Where,}$$

m is the mass (kg)

r is the circle radius of projected mass (m)

ω is the angular velocity of the projected mass (rad/s).

The weight, W_t of each projected mass was calculated as the product of mass, m (kg), and acceleration due to gravity, g (m/s²). The spring stiffness, k was calculated as $Gd^4/8D^3$. Where,

G is the shear modulus of spring material

d is wire diameter (mm)

D is the spring mean diameter (mm).

Pretension force of the spring, $F_s = k \cdot \delta s$.

δs = free length - pretension length

$$= 64 - 37.5 = 26.5 \text{ mm}$$

$$F_s = 0.2 \times 26.5 = 5.3 \text{ N.}$$

Spring pretension force, $F_s = 5.3 \text{ N}$

This pretension force must balance the weight of the projected mass, W_t , and the centrifugal forces generated by the projected mass $F_c(250)$ below the nominal rotor speed of 250 rpm [15].

I.e. pretension force, $F_s = W_t + F_c(250)$

$$5.3 = mg + m\omega^2 = m(g + \omega^2)$$

The radius, r of the projected masses is 0.09 m.

$$5.3 = m(g + r(2\pi n/60)^2) = m(9.81 + 0.09(2 \times 3.142 \times 250/60)^2) = m \times 71.495$$

$$5.3 = m \times 71.495$$

$m = 5.3/71.495 = 0.0741 \text{ kg}$, the mass of the projected masses, $m \approx 74 \text{ g}$.

Weight of projected mass, $W_t = 0.074 \times 9.81 = 0.726921 \text{ N} \approx 0.7 \text{ N}$.

Centrifugal forces generated at 250 and 300

rpm respectively, are:

$$F_c(250) = 0.0741 \times 0.09(2 \times 3.142 \times 250/60)^2 = 4.6 \text{ N}$$

$$F_c(300) = 0.0741 \times 0.09(2 \times 3.142 \times 300/60)^2 = 6.6 \text{ N.}$$

From equation (1), for a rising blade the available pitching force, F_R at 300 rpm of the rotor is obtained as: $F_R = F_c + W_t - F_s$ ---- (1)

$$= 6.6 + 0.7 - 5.3 = 2$$

$$F_R = 2 \text{ N.}$$

The optimal pitch angle, ϕ as determined from experiment no. 1 is 35°. The spring stroke that defines the linear displacement of the cam follower as the blade pitches between 35° and 0° is 5mm; therefore pitch degree per linear displacement of the cam follower is 7°.

I.e. $35/5 = 7^\circ/\text{mm}$.

Spring rate, $k = 0.2 \text{ N/mm}$. The spring stroke force to maximum pitch is the spring rate, $k \times \text{stroke} = 0.2 \times 5 = 1 \text{ N}$.

Since the stroke force is 1 N, F_R being 2 N means that a surplus pitch force of 1N which is partly restricted by a stopper exists as the blade's pitch angle is reduced to 0°.

At 250 rpm, $F_R = 4.6 + 0.7 - 5.3 = 0 \text{ N}$,

As such blade pitching will not start until the rotor speed exceeds 250 rpm.

For a falling blade, the available pitching force, F_F at 300 rpm of the rotor is obtained from equation (2) as follows:

$$F_F = F_c - W_t - F_s \text{ ---- (2)}$$

$$= 6.6 - 0.7 - 5.3 = 0.6$$

$$F_F = 0.6 \text{ N}$$

But the force needed to pitch the blade completely to 0° i.e. stroke force for 5 mm is 1 N. This translates to 0.2 N per mm stroke. F_F being 0.6 N is only 60% of the stroke forces. $0.6 \text{ N} \div 0.2 \text{ N/mm} = 3 \text{ mm stroke}$. As calculated earlier 1 mm stroke = 7° pitch. $7^\circ \times 3 = 21^\circ$ pitch. Therefore a falling blade may only pitch up to 21° or 60% of the aggregate pitch angle, i.e. $0.6 \times 35^\circ = 21^\circ$ (21° away from 35°) or, $35^\circ - 25^\circ = 14^\circ$ (14° towards 0°).

The mass, m of the projected 74 g, at 90 mm rotational radius generates 6.6 N to pitch a blade to an angle of attack where pitch angle ϕ is 0° or 14° during rising and falling conditions respectively, at 300 rpm.

Experiment no.2 was conducted to test the performance of the stall control mechanism of the wind turbine below and above the rated wind speed of 11m/s. The data obtained from this experiment are the wind speed (m/s), rotor speed (rpm), generator output voltage (volt), and generator output current (mA). The relationship between wind speeds and generator output power indicates if the turbine has experienced a stall condition during the test.

Solidworks motion analysis feature was used to analyze the pitching action of the wind turbine model at the maximum rotor speeds (rpm) obtained when the turbine was tested during experiment no. 2.

The pitch to stall power curve plotted from the table of results in experiment no.2, which shows the relationship between the wind speed and power output, as well as the motion analysis simulation result, was observed in concluding the performance effect of the stall control mechanism.

Below are the pictures of the prototype wind turbine during experiments in the wind tunnel of the power machines laboratory, electrical engineering department Kaduna polytechnic Nigeria.



Plate 1: Assembled Rotor and Measuring Instruments



Plate 2: Prototype Front View



Plate 3: Prototype Isometric View



Plate 4: Turbine in the Wind Tunnel (back view)

III. RESULTS

Experiment no. 1: Determination of optimal pitch angle and the critical angle of attack.

Table 2 below contains data obtained from the experiment to determine the optimal pitch angle at 11 m/s wind speed.

Table 2: Optimum pitch angle determination result

Pitch angle, β ($^{\circ}$)	Rotor speed (rpm)	The angle of attack, $\alpha = (\phi - \beta)$ ($^{\circ}$)
20	223	19
25	235	14
30	275	9
35	300	4
40	235	-1
45	195	-6

At 35° pitch angle, the turbine experienced the fastest rotational speed at the rated wind speed of 11 m/s. below and above 35° the rotor speed drops, as such this angle was considered the optimal pitch angle of the NACA 9912 airfoil used for the rotor blades.

The angle ϕ (°) is calculated as presented below:

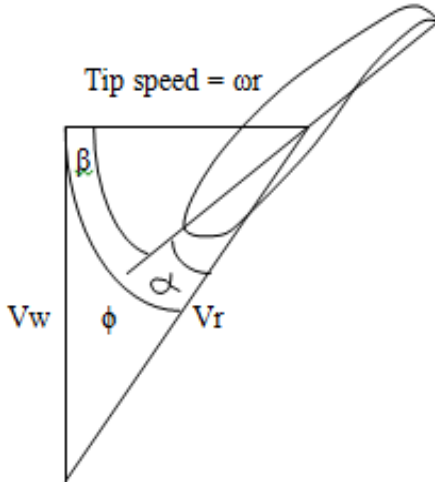


Figure 6: Wind Velocity Triangle

$$\phi = \tan^{-1} V_w / \omega r \text{ where,}$$

$$V_w = \text{wind speed (m/s)}$$

$$\omega = \text{angular velocity (rad/s)}$$

$$r = \text{radius of rotor (mm)}$$

$$\phi = \tan^{-1} (11 \times 60) / 2\pi n r$$

$$= \tan^{-1} (660 / 2.7335n) \text{ where,}$$

$$n = \text{rotor speed (rpm)}$$

$$\phi = \tan^{-1} (241.4487/n).$$

At 300 rpm,
 $\phi \approx 39^\circ$

EXPERIMENT NO. 2: Stall Mechanism Performance Test.

Table 3: Turbine performance test data

Wind speed (m/s)	Rotor speed (rpm)	Generator voltage (v)	Generator current (mA)	Output power (mW)
3	65	2.90	7.02	20
4	82	3.90	9.00	35
5	135	6.00	14.00	84
6	194	8.10	17.30	140
7	210	10.60	21.40	227
8	230	10.70	26.00	278
9	256	11.10	26.70	296
10	269	11.40	28.10	320
11	271	11.50	29.10	322
12	245	10.90	26.70	291
13	240	10.60	26.50	281
14	243	10.70	26.60	285

Table 3 above contains experimental data obtained during the stalled mechanism performance test conducted on the prototype wind turbine in a wind tunnel. The data was used to plot the pitch to stall power curve below, which is an ideal indicator for the power limit at which the machine can stall the turbine and prevent it from over speeding.

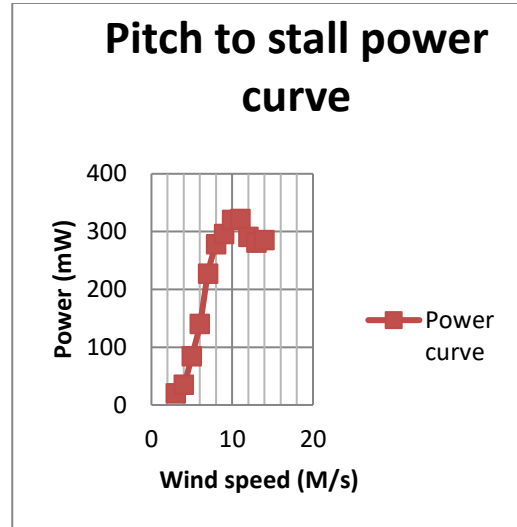


Figure 7: Pitch to Stall Power Curve

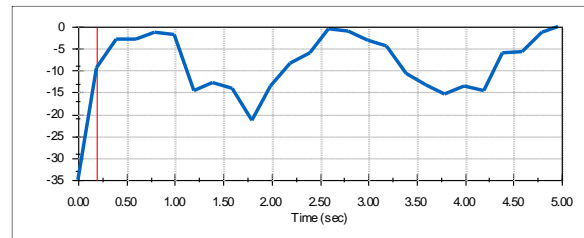


Figure 8: Graph of pitch action at maximum rotor speed (showing pitch action where $\beta \approx 10^\circ$ during rising).

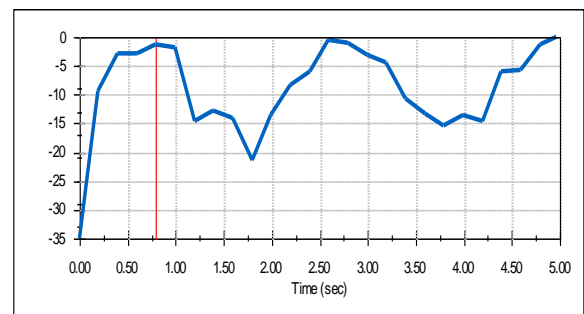


Figure 9: Graph of pitch action at maximum rotor speed (showing pitch action where $\beta \approx 1^\circ$ during rising).

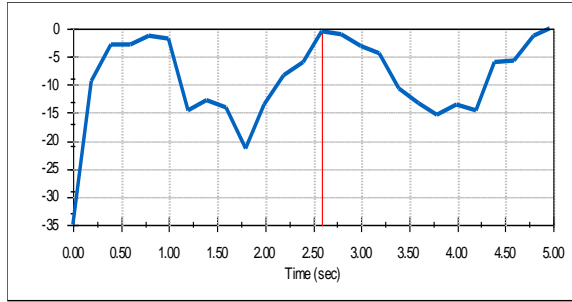


Figure 10: Graph of pitch action at maximum rotor speed (showing maximum pitch action where, $\beta = 0^\circ$ during rising).

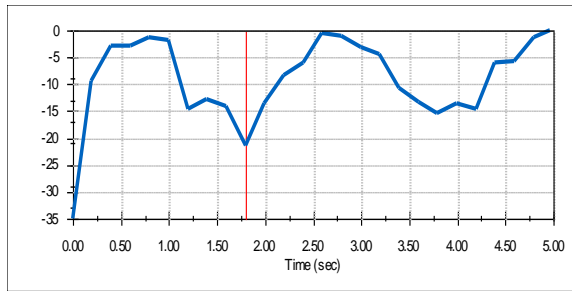


Figure 11: Graph of pitch action at maximum rotor speed (showing pitch action where $\beta = 20^\circ$ during fall).

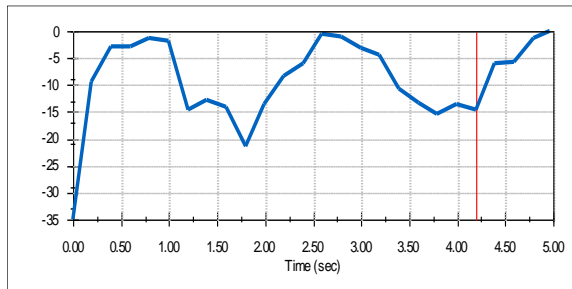


Figure 12: Graph of pitch action at maximum rotor speed (showing pitch action where $\beta = 15^\circ$ during fall).

IV. DISCUSSION

The pitch to stall power curve figure 7 above shows that the turbine began to stall at about 11 m/s wind speed, after achieving a maximum rotor speed of 271 rpm as indicated in table 3 above. The pitch angle curve obtained from the motion analysis simulation result at the same rotor speed agrees with this stall behavior, as blades pitch angle instantaneously changed linearly from 35° to about 10° within approximately 0.2 sec of the simulation (figure 8), thereby significantly increasing the angle of attack of the airfoils. The pitch angle then subsequently changed to about 1° and finally 0° after about 0.8 sec and 2.6 sec respectively during rising (figure 9 & 10) and to about 20° and 15° after about 1.8 sec and 4.2 sec during fall (figure 11 & 12). The 0° and 15° pitch angles observed in the simulation result are essentially the same as the calculated values in the theory,

with a difference of just 1° in the blade fall condition which was theoretically 14° . The blades have likely maintained periodically the pitch angles of 0° and 15° during rising and fall conditions respectively as the rotor assembly continued to rotate at 271 rpm. The difference in the pitch angle between the rise and fall conditions of the blades is a result of the directional effect of weights of the projected masses which always act downward. And this may as well, given the possibility for further over-speed control, since a falling blade will pitch further towards 0° pitch angle if the rotor should tend to rotate at higher speeds under a more severe wind condition.

The power curve (figure 7) shows a cut-in speed of about 3 m/s in region 1, for the wind turbine, with the control mechanisms mounted on the rotor, which consequently increases the inertia of the rotor assembly. A lower cut-in speed would have been the case if the speed control mechanism was excluded from the rotor assembly or if the rotor diameter is increased [18]. Region 2 is the power optimization region where the rotor speed, as well as power production, are proportional to the wind speed. In region 3 the rotor speed and power are maintained at constant mean values where the pitch angle of the blades keeps on changing within a specific range of 0° and 15° during rising and fall conditions respectively [17].

The profile of the power curve showed a reasonable rotor as well as power stability even though a rising blade pitches higher than a falling blade due to the directional effect of weights of the projected masses which always acts downwards as stated earlier. This is an indication of a compensatory effect on the rotor, occurring between a rising blade and a falling blade since both conditions occur simultaneously.

V. CONCLUSION

The results above showed that the simple stall control mechanism was able to stall the prototype wind turbine at about 11 m/s wind speed when experimented for a wind speed range of 3 m/s to 14 m/s, and the turbine produced a power curve closely similar to an ideal pitch to stall power curve.

Acknowledgments

This work is based on a research support scheme by the Tertiary Education Trust Fund (Tetfund) Nigeria grant. Acknowledgment also goes to Engr. Hassan Salau of the department of electrical engineering Kaduna polytechnic, Nigeria his technical contributions in executing the project.

REFERENCES

- [1] (GWEC), G. W. (2018). Global Wind Report, Brussels, Belgium: GWEC.
- [2] Gorgulu Y. F., Ozgur M. A., Kose R., Wind Turbine Applications in Doha Metro, Qatar. SSRG International Journal of Mechanical Engineering, 7(2) (2020) 21-25.
- [3] Liu X., Liang S., Li G., Godbole A., Lu C. An improved dynamic stall model and its effect on wind turbine fatigue load

- Prediction, Renewable Energy. (2020) 117-130.
- [4] Archer C. L., Jacobson M. Z. Evaluation of Global Wind Power, Journal of Geophysical Research, D12110 (2005)..
- [5] Li Y., Paik K-J., Xing T., Carrica P. M Dynamic overset CFD simulation of wind turbine aerodynamics, Renewable Energy. (2012) 285-298.
- [6] Dai J. C., H. Y.. Aerodynamics loads calculation and analysis for large scale wind turbine based on combining BEM modified theory with dynamic stall model. Renewable Energy, (2011) 1095-1104.
- [7] Bak, C. Aerodynamic Design of Wind Turbine Rotors. Woodhead Publishing Series in Energy. (2013) 59-108.
- [8] Bossanyi E. Individual Blade Pitch Control for Load Reduction. Wind Energy. (2003) 119-128.
- [9] Ragheb, M. (2016, 4 24). Control of Wind Turbines. p. 2.
- [10] Venkaiah P., Sarkar B. K, Hydraulically actuated horizontal axis wind turbine pitch control by model-free adaptive controller, Renewable Energy. (2020) 55-68.
- [11] Xu Y., Peng Y., Zhan S. (2019). Optimal blade pitch function and control device for high-solidity straight-bladed vertical axis wind turbine, Applied Energy. 1613-1625
- [12] Oyewole, J., & Aroto. Wind Speed Pattern in Nigeria (A Case Study of Some Coastal and Inland Areas). JASEM ISSN 1119-8362, (2018) 119-123.
- [13] Tang, X. (2012, September). Aerodynamic Design and Analysis of Small Horizontal Axis Wind Turbine Blades. Central Lancashire, Preston, UK.
- [14] Sudhamshu A.R., M. C. Numerical study of the effect of pitch angle on performance characteristics of a HAWT. Engineering Science and Technology, an International Journal. (2016) 632-641.
- [15] Kang, M. C. (2010). Patent No. 12/906,100. The United States of America.
- [16] Madan Kumara M C, Nandish. R. V, Madhu E,S Ramachandra, Fatigue Failure Analysis of Twisted Blade, SSRG International Journal of Mechanical Engineering 1.3 (2014) 11-15.
- [17] Thomas Esbensen, B. T. Joint Power and Speed Control of Wind Turbines. Alborg, Denmark: AALBORG UNIVERSITY (2008).
- [18] Jose F. Herbert-Acero, J. M.-L.-D.-R.-E.-V. Aerodynamic Optimization of Small Wind Turbine Rotors Based on NACA 4-Digit Airfoils Through Computational Intelligence. European Wind Energy Conference & Exhibition 2014. Fira de Barcelona Gran Via, Spain.: The European Wind Energy Association (EWEA) (2014).